Proceedings of the 11th World Congress on Electrical Engineering and Computer Systems and Sciences (EECSS'25)
Paris, France – August, 2025
Paper No. ICBES 187
DOI: 10.11159/icbes25.187

Prediction of the Shape of Severely Fractured Distal Tibia by Using Statistical Shape Modelling

Athena Jalalian, Soheil Arastehfar, Ian Gibson
University of Twente
Drienerlolaan 5, 7522 NB, Enschede, Netherlands
a.jalalian@utwente.nl; s.arastehfar@utwente.nl

Abstract **-** The design of tibial components of ankle implants is critical for proper functioning. The tibial component design uses the shape of the distal tibial bone as reference. However, when the distal tibia is severely damaged or fractured, the design of tibial components becomes very difficult. In this paper, we aim to study prediction of the distal tibia shape based on the remainder of tibial bone. We use statistical shape modelling technique to create a model of the tibial bone, and then we assess its shape variability. We extract the relationships between the shape variations to produce the predictions. A dataset of 22 female bone samples and 30 male bone samples were acquired. A statistical shape model per gender was produced by using a part of the dataset population. The first set of principal component analysis modes accounted for at least 95% of the shape variations were adopted. For the rest of the bone samples, we attempted to predict their distal tibia shapes by feeding the shapes of their proximal tibia and tibial shafts into the models. The prediction was done for roughly up to 20 mm above the distal tibial articular surface. The study was done in a 5-fold cross validation setting. Root-mean-square errors of reconstruction of the samples excluded in the model development were 1.91 ± 0.61 mm and 2.01 ± 0.39 mm for females and males, respectively. The prediction errors of the distal tibia, when only the shape of the proximal tibia and tibial shafts were known, were in average 1.96 mm for female's bones and 2.46 mm for male's bones. These small errors can show that the distal tibia shape can be reconstructed based on the proximal and shaft shapes. This is a preliminary result bringing new insights into treatment of ankle orthopaedic diseases. It can pave the way for reconstruction of lost distal tibia.

Keywords**:** distal tibia, ankle implant design, statistical shape modelling, shape prediction

1. Introduction

Distal tibia plays a crucial role in ankle stability and weight-bearing. In the ankle joint, the distal tibia articulates with the talus bone and the fibula, to form part of the joint enclosure contributing to its stability. The distal tibia widens towards its lower end to assist with weight-bearing. Such essential functions show the importance of proper replacement of the distal tibia with implants in treatment of ankle orthopaedic diseases [1]. For example, in total ankle arthroplasty for treatment of end-stage ankle arthritis [2], the damaged distal tibia is replaced by a metallic implant to bring comparable stability and weight-bearing performance.

In tibial components of ankle implants, maximization of distal tibia coverage is essential [3]. As such, detailed measurements of the anatomy of distal tibia are required. Current clinical evaluation methods rely on radiographic images [4]. After defining the anatomic landmarks on the images, geometric parameters such as distances, angles, or areas are measured to describe the bone anatomy [5-7]. However, for patients with pathological changes in the tibia, e.g. fracture, anterior impingement and osteochondral lesions, we need to find an alternative to the measurements.

Given the complexity of the shape variations of the distal tibia [8, 9], we need a robust analytical tool to analyse its anatomy. Statistical shape modelling (SSM), by using a dataset of radiographs, can construct a three-dimensional (3D) mean shape of a bone and its variations to represent its anatomy [10, 11]. Yu et. al [4] created an SSM of the 10-mm resection surface of the distal tibia to study the shape variability for implant design. Using the mean shape and the first seven modes of the principal component analysis, they constructed a distal tibia shape model. They found the anterior–posterior and medial–lateral distances as the main sources of variation.

SSM techniques can help with prediction of the anatomical information through identification of morphological similarities and differences in a population of tibia bone samples [12, 13]. As such, when the measurement of distal tibia is

not possible, e.g. due to its fracture, we might be able to predict its 3D shape by using an SSM model and the remaining of the bone, e.g. proximal tibia and tibial shaft. However, this is yet to be studied.

In this paper, we aim to determine if, for a tibia bone, the shape of its distal end can be predicted given its proximal end and shaft. We used SSM techniques to create a 3D shape model of tibia and adopted the model for the prediction. In section 2, we introduce the study design. Section 3 presents the results following a discussion. We conclude the paper in section 4.

2. Study Design

An overview of our study is depicted in Figure 1. A dataset of 3D tibia bones was available for this study. We created 3D models of the tibia bone by using SSM techniques for each gender separately due to their significant shape differences [8, 9]. The bone dataset was split into 5 subsets. An SSM model was produced by using four of the subsets and tested for its prediction capability on the fifth subset. For the prediction purpose, we removed 25%, 50%, 75%, and 100% of the distal ends of the bones in the fifth subset. In addition, we attempted to reconstruct the bones included in and excluded from the SSM modelling step to form a benchmark. Root-mean-square errors (RMSE) were used to compare the result and evaluate the prediction capability of the models. The above process was done 5 times in a 5-fold cross validation setting.

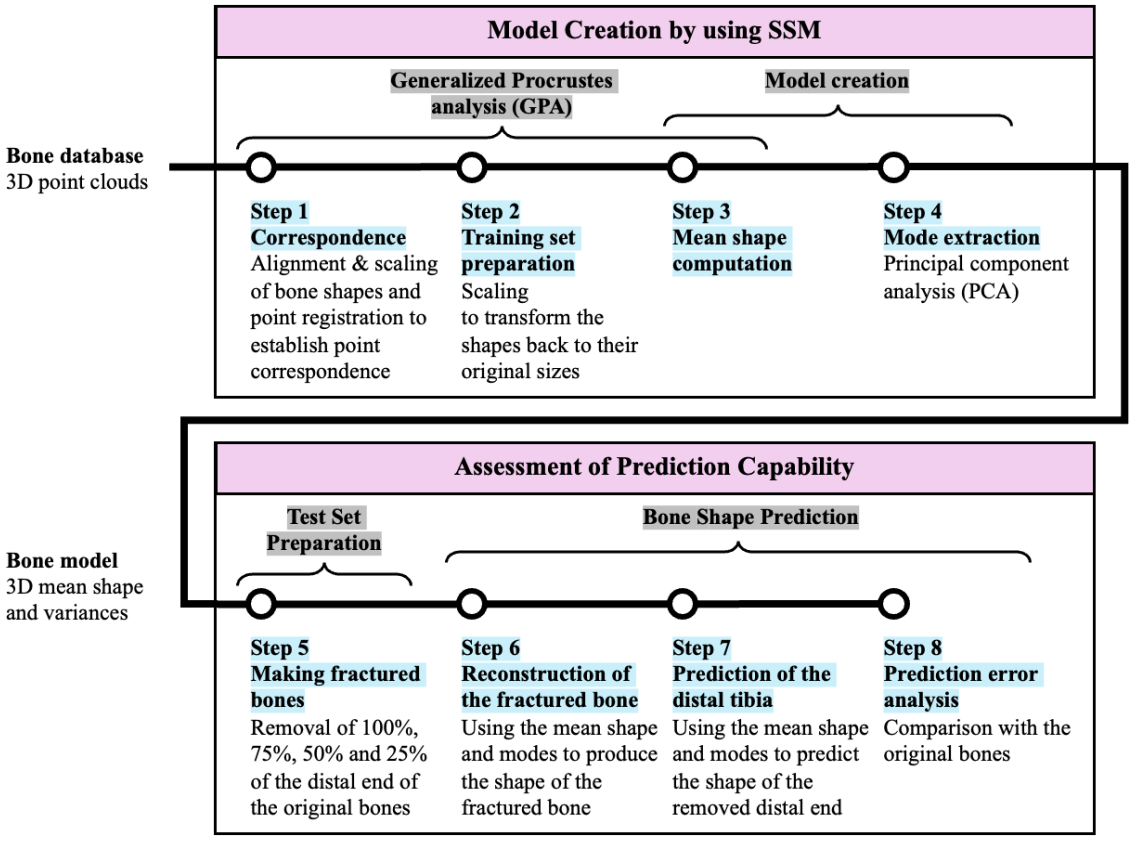

Fig. 1: Overview of the study design and workflow.

2.1. Datasets

The dataset was acquired from (https://github.com/MCM-Fischer/VSDFullBodyBoneModels) [14]. It contained the left and right bones of 11 female and 15 male subjects. The left bones were mirrored to form a 22 female bone set and 30 male bone set. The descriptive data of the subjects is presented in Table 1. The female subjects aged 48 ± 16 years. Their weight

and height were 61.2 ± 15.3 kg and 1.7 ± 0.1 m. The male subjects were 57 ± 21 years old, weighed 78.1 ± 6.3 kg, and had height of 1.8 ± 0.1 m.

Table 1: Descriptive data of the subjects.

No.	Gender	Age	Weight	Height
1	F	72	80.2	1.72
2	F	39	37.4	1.8
3	F	61	53.4	1.69
4	F	30	50.46	1.68
5	F	37	50.5	1.69
6	F	47	61	1.66
7	F	41	56.3	1.65
8	F	30	65	1.65
9	F	45	54	1.65
10	F	51	90	1.77
11	F	78	75	1.62
12	M	43	76.95	1.78
13	M	26	81.8	1.87
14	M	83	75	1.73
15	M	84	75.4	1.67
16	M	34	87	1.79
17	M	38	72	1.8
18	M	58	71.3	1.81
19	M	25	74	1.75
20	M	65	82.3	1.77
21	M	76	87	1.8
22	M	74	86	1.82
23	M	56	68	1.7
24	M	81	78	1.75
25	M	48	NA	NA
26	M	69	NA	NA

2.2. Models

The bone models were defined as the mean shape and its modes. An estimate of a 3D bone shape is given by Eq. (1).

$$\boldsymbol{X} \approx \hat{\boldsymbol{X}} = \left\{ \hat{x} = U + \sum_{j=1}^{m} \alpha_j M_j / \alpha_j \in \mathbb{R}, -3 \leq \alpha_j \leq 3 \right\} \tag{1}$$

Where, $\boldsymbol{X}$ and $\hat{\boldsymbol{X}}$ are the bone shape and its estimate respectively. U is the mean shape and M denotes the modes. m defines the number of modes accounting for at least 95% of the variations. α is the mode coefficient and is varied from -3 to 3 to define the range containing 99.7% of the bone population according to the 3-sigma rule.

3. Results and Discussion

Five SSM models were produced for the female bones and 5 for the male bones. The steps of the generalized Procrustes analysis (GPA) in Figure 1 with bone visualizations are shown in Figure 2. Figure 2a shows all the bones together. In the first step, the bones were aligned via rigid transformations and scaling to produce a general bone shape (Figure 2b). These bones were translated, rotated, and scaled to match their shapes with the least RMSE to form a general bone shape. Then, non-rigid transformations were applied to make the shapes of all the bone samples as close as possible (Figure 2c). Next, point registration was applied based on nearest neighbour to establish correspondence (Figure 2d). After that in step 2, the bones were scaled back to their original size to prepare the bones for model creation (Figure 1e). On these bones, the average shape was computed (step 3), and then principal component analysis (step 4) was applied for mode (variance) extraction. These bone samples contained 7.77e3 ± 1.47e3 3D datapoints, and 700 points (almost 10%) were registered for the mean shape and modes.

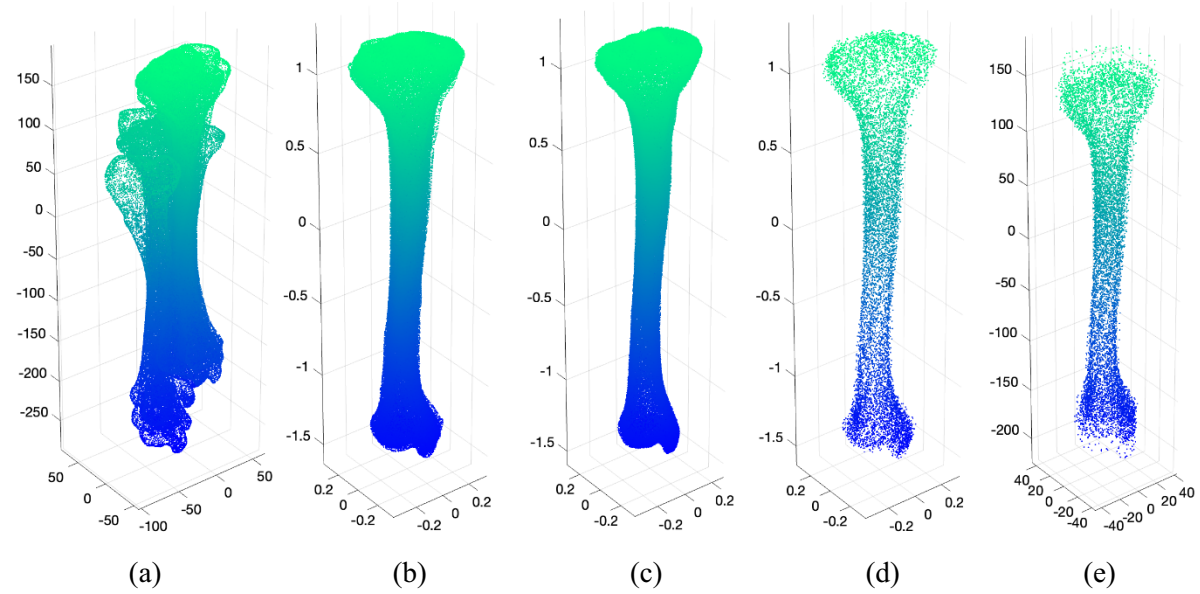

Fig. 2: Illustration of the steps of GPA with an example bone, (a) all the bones, (b) bones after alignment via rigid transformation and scaling, (c) bones after non-rigid transformation, (d) bones after point registration and correspondence establishment, (e) bones after reverting the scales

RMSEs of the models for representing the bones included in model development were 1.58 ± 0.39 mm and 1.92 ± 0.35 mm, respectively. These small errors could show that the models could represent the sample bones successfully. As for the excluded bones, the RMSEs were 1.91 ± 0.61 mm and 2.01 ± 0.39 mm for females and males, respectively. These errors were comparable to those of the included bones, which can imply the model effectiveness at production of a bigger population of bones. In average, seven modes represented greater than 95% of the variations for both female's and male's bones.

The prediction errors were slightly higher than the model RMSEs after removing fractions of distal tibia for both females and males (Figures 3 and 4). Despite this, they were within the acceptable range referring to the errors reported in [4]. An interesting finding is that the prediction errors changed very slightly when increasing the removal percentage. This might indicate that the shapes of the proximal tibia and tibial shafts are good enough for prediction of the distal end. As such, the 3D shape of severely fractured or damaged tibia can still be predictable by using SSM models if the shape of the remaining of tibia bones can be acquired. This has a significant clinical implication that implant designs for distal tibia is affected by fewer shape parameters and thus less design variations are needed for the implants.

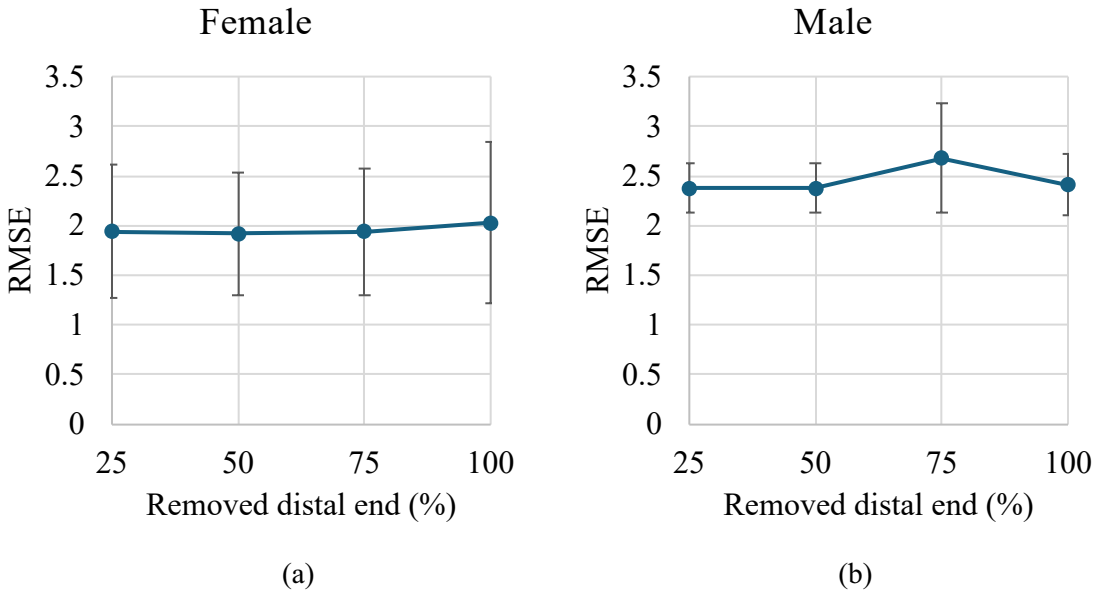

Fig. 3: Prediction errors of the bones after removal of 25%, 50%, 75% and 100% of the distal end.

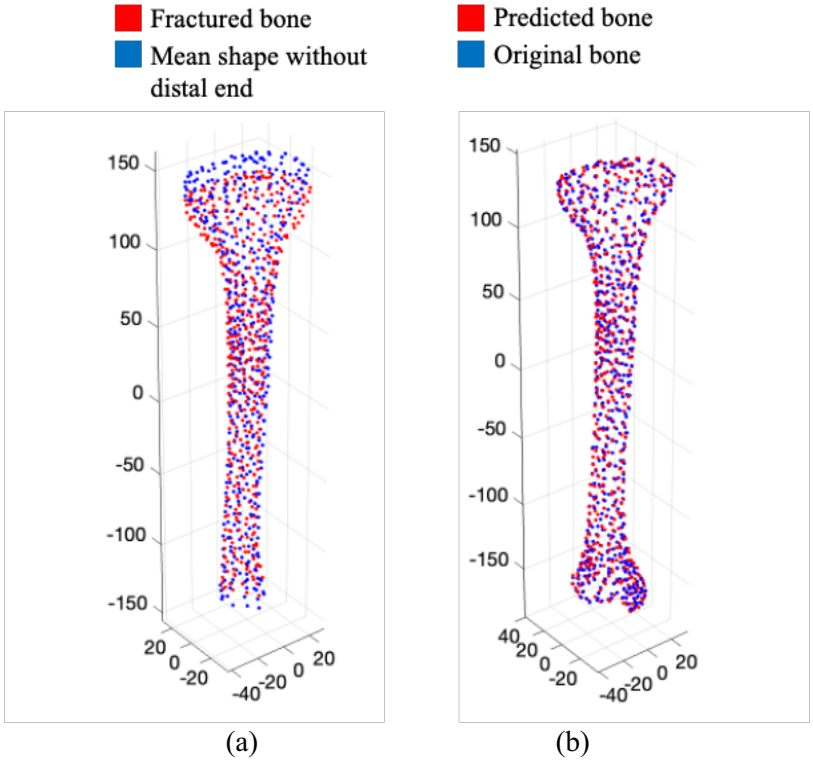

Fig. 4: Illustration of an original tibia with removed distal end, the reconstructed bone shape, and comparison with the original bone, (a) the remaining of the bone after removing the distal tibia plotted on the similar fraction of the mean shape, (b) the predicted full bone projected on the original full bone.

4. Conclusion

This study showed that the shape of distal tibia can be predicted given the shape of the proximal tibia and tibial shafts. This finding is extremely clinically relevant as it implies that proper implants can still be designed even if the distal tibia is severely fractured or damaged. However, this was a preliminary study to test the feasibility of SSM models for providing such predictions. Further study on a bigger dataset is required to explain the morphology of the distal tibia. In addition, the significance of each mode for shape prediction can be investigated so that the implants can be designed by focusing on the parameters that affect the shape more.

References

[1] C. L. Brockett and G. J. Chapman, "Biomechanics of the ankle," *Orthopaedics and trauma,* vol. 30, no. 3, pp. 232-238, 2016.

[2] S. M. Raikin, M. R. Rasouli, R. Espandar, and M. G. Maltenfort, "Trends in treatment of advanced ankle arthropathy by total ankle replacement or ankle fusion," *Foot & Ankle International,* vol. 35, no. 3, pp. 216-224, 2014.

[3] C. E. Gross, A. A. Palanca, and J. K. DeOrio, "Design rationale for total ankle arthroplasty systems: an update," *JAAOS-Journal of the American Academy of Orthopaedic Surgeons,* vol. 26, no. 10, pp. 353-359, 2018.

[4] J. Yu, C. Li, J. Lyu, S. Cao, C. Zhang, X. Ma, and D. Zhao, "Statistical shape modeling of shape variability of the human distal tibia: implication for implant design of the tibial component for total ankle replacement," *Frontiers in Bioengineering and Biotechnology,* vol. 13, p. 1504897, 2025.

[5] J. Yu, D. Zhao, S. Wang, P. Chu, C. Zhang, J. Huang, X. Wang, and X. Ma, "Finite element analysis of the biomechanical effect of bone resection depth in the distal tibia after total ankle replacement," *Journal of Medical and Biological Engineering,* vol. 42, no. 4, pp. 422-428, 2022.

[6] C. V. Nguyen, J. D. Greene, D. R. Cooperman, and R. W. Liu, "An anatomic and radiographic study of the distal tibial epiphysis," *Journal of Pediatric Orthopaedics,* vol. 40, no. 1, pp. 23-28, 2020.

[7] C.-C. Kuo, H.-L. Lu, T.-W. Lu, A. Leardini, M.-Y. Kuo, and H.-C. Hsu, "Validity and reliability of ankle morphological measurements on computerized tomography-synthesized planar radiographs," *Biomedical engineering online,* vol. 15, pp. 1-16, 2016.

[8] L. Claassen, P. Luedtke, D. Yao, S. Ettinger, K. Daniilidis, A. Nowakowski, M. Müller-Gerbl, C. Stukenborg-Colsman, and C. Plaass, "Ankle morphometry based on computerized tomography," *Foot and Ankle Surgery,* vol. 23, p. 121, 2017.

[9] M. B. Ataoğlu, M. A. Tokgöz, A. Köktürk, Y. Ergişi, M. Y. Hatipoğlu, and U. Kanatlı, "Radiologic evaluation of the effect of distal tibiofibular joint anatomy on arthroscopically proven ankle instability," *Foot & Ankle International,* vol. 41, no. 2, pp. 223-228, 2020.

[10] T. Heimann and H.-P. Meinzer, "Statistical shape models for 3D medical image segmentation: a review," *Medical image analysis,* vol. 13, no. 4, pp. 543-563, 2009.

[11] A. L. Lenz, N. Krähenbühl, A. C. Peterson, R. J. Lisonbee, B. Hintermann, C. L. Saltzman, A. Barg, and A. E. Anderson, "Statistical shape modeling of the talocrural joint using a hybrid multi-articulation joint approach," *Scientific Reports,* vol. 11, no. 1, p. 7314, 2021.

[12] P. M. Mitchell, K. A. Harms, A. K. Lee, and C. A. Collinge, "Morphology of the posterior malleolar fracture associated with a spiral distal tibia fracture," *Journal of orthopaedic trauma,* vol. 33, no. 4, pp. 185-188, 2019.

[13] R. Blom, D. Meijer, R. O. de Muinck Keizer, S. Stufkens, I. Sierevelt, T. Schepers, G. Kerkhoffs, J. Goslings, and J. Doornberg, "Posterior malleolar fracture morphology determines outcome in rotational type ankle fractures," *Injury,* vol. 50, no. 7, pp. 1392-1397, 2019.

[14] M. C. Fischer, "Database of segmentations and surface models of bones of the entire lower body created from cadaver CT scans," *Scientific Data,* vol. 10, no. 1, p. 763, 2023.